Geochemistry Geophysics Geosystems G3
AN ELECTRONIC JOURNAL OF THE EARTH SCIENCES
Published by AGU and the Geochemical Society

Article
Volume 1
Published July 11, 2000
Paper number 1999GC000012
ISSN: 1525-2027

Spatial distribution of melt conduits in the mantle beneath oceanic spreading ridges: Observations from the Ingalls and Oman ophiolites

Peter B. Kelemen, Michael Braun, and Greg Hirth

Woods Hole Oceanographic Institution, Woods Hole, Massachusetts 02543 (peterk@whoi.edu; mbraun@whoi.edu; ghirth@whoi.edu)

[1] **Abstract:** Ophiolites are on-land exposures of igneous crust and residual upper mantle formed beneath submarine spreading ridges. Upper mantle outcrops in ophiolites provide insight into focusing of melt transport from a ~100 km wide region of partial melting into an ~5 km wide zone of igneous crustal accretion beneath the ridges. Dunite veins, composed of the minerals olivine and spinel, mark conduits for melt transport through at least the uppermost 30 km of the mantle. New data in this paper, on dunite veins in the Ingalls ophiolite, central Washington Cascades, show a power law relationship between frequency and width, in which frequency/m ≈ 0.02 width^{-3} over a size interval from ~0.1 to 2 m. There may be several ways to generate this relationship, but we favor the hypothesis that the dunites represent a coalescing melt transport network. This conclusion is broadly consistent with the related hypothesis that mantle melt extraction occurs in a fractal, branching network, and with recent results on formation of a coalescing network of dissolution channels via flow of a solvent through a partially soluble, compacting porous medium.

Keywords: Melt; transport; mid-ocean ridge; mantle; dunite.

Index Terms: Midocean ridge processes; physics of magma and magma bodies; magma migration; fractals and multifractals.

Received September 3, 1999; **Revised** May 1, 2000; **Accepted** June 6, 2000; **Published** July 11, 2000.

Kelemen, P. B., M. Braun, and G. Hirth, 2000. Spatial distribution of melt conduits in the mantle beneath oceanic spreading ridges: Observations from the Ingalls and Oman ophiolites, *Geochem. Geophys. Geosyst.*, vol. 1, Paper number 1999GC000012 [8266 words, 8 figures, 1 table]. Published July 11, 2000.

1. Introduction

[2] There are two essential observational constraints on melt extraction from the mantle beneath oceanic spreading ridges. (1) Primitive mid-ocean ridge basalts (MORB) are not in equilibrium with shallow, residual mantle peridotites with the mineral assemblage olivine + orthopyroxene (opx) + clinopyroxene (cpx) + spinel [*O'Hara*, 1965; *Stolper*, 1980]. (2) Melt transport occurs via mechanisms that produce coalescence from a broad melting region toward the narrow zone beneath the ridge axis where igneous crust is formed. Below, we examine these constraints in more detail.

[3] MORB, and other basalts from submarine spreading ridges (e.g., ophiolites and back arc

basins), are far from saturation in opx, whereas opx is an abundant mineral in residual mantle peridotites extending upward to the base of the igneous crust. The composition of partial melts equilibrated with mantle peridotites changes with pressure, so that melts formed at a relatively high pressure are saturated only in olivine ± spinel at a lower pressure. While MORB is a mixture of liquids equilibrated with peridotite at a variety of different depths, its composition is strikingly similar worldwide, so the mixing proportions must be nearly constant. In this context, MORB has a composition consistent with equilibration with mantle peridotite at an average depth greater than 30 km below the seafloor. In addition, dissolution of opx in opx-undersaturated mantle melts is kinetically very rapid [*Brearley and Scarfe*, 1986; *Kuo and Kirkpatrick*, 1985a, 1985b]. Thus the fact that MORB is undersaturated in opx provides a strong constraint on melt transport. For the average depth of equilibration to be greater than 30 km most liquids parental to MORB must pass through at least the top 30 km of the upper mantle without equilibrating with opx in residual mantle peridotite. Trace element disequilibrium between residual peridotites and MORB provides a similar constraint [*Johnson et al.*, 1990; *Spiegelman and Kenyon*, 1992]. These constraints can be satisfied by (1) very rapid transport, for example in melt-filled fractures [*Nicolas*, 1986] (so that the diffusion time is short) or (2) by slower, porous flow in wide, dunite conduits, in which the distance between migrating melt and opx in residual peridotite is longer than the diffusion distance [*Kelemen et al.*, 1997, 1995a, 1995b]. For melt transport times through the upper 30 km of the upper mantle of 3000 to 30,000 years and effective diffusivity $\sim 5 \times 10^{-12}$ m^2/s (melt diffusivity $\sim 10^{-10}$, porosity ~ 0.05), this requires dunite widths greater than 0.7 to 2 m.

[4] Focusing of melt from a broad melting region toward the narrow zone beneath the ridge axis is apparent because (1) igneous ocean crust at fast-spreading ridges reaches 95% of its total thickness within 2 km of the ridge axis [*Vera et al.*, 1990], and (2) theory and seismic data suggest that the region of partial melting is of the order of 100 km wide at its base [*Bottinga and Allegre*, 1973; *Forsyth et al.*, 1998; *Langseth et al.*, 1966]. Melt extraction in fractures spanning the melting region in mantle undergoing passive, corner flow beneath a spreading ridge cannot satisfy this constraint, because such fractures, formed parallel to the direction of maximum compressive stress, would reach the top of the mantle over a region more than 80 km wide [*Sleep*, 1984]. Instead, focusing of melt extraction in a narrow region beneath the ridge axis requires either (1) very highly focused solid mantle upwelling [*Buck and Su*, 1989; *Jousselin et al.*, 1998; *Nicolas and Rabinowicz*, 1984; *Rabinowicz et al.*, 1984], or (2) a variety of porous flow mechanisms including "suction" due to corner flow [*Phipps Morgan*, 1987; *Spiegelman and McKenzie*, 1987]; anisotropic permeability along mineral foliation [*Phipps Morgan*, 1987] or in stress controlled planes of high porosity [*Daines and Kohlstedt*, 1997; *Zimmerman et al.*, 1999]; channels at the base of the "lithosphere," beneath a permeability barrier created by melt crystallization [*Sparks and Parmentier*, 1991; *Spiegelman*, 1993]; and coalescence of dissolution channels forming as a result of reactive porous flow [*Aharonov et al.*, 1995; *Kelemen et al.*, 1995b; *Spiegelman et al.*, 2000].

[5] Minerals in dunites in the mantle section of the Oman ophiolite have compositions that are close to chemical equilibrium with MORB and with similar basalts from other submarine spreading centers (e.g., ophiolites, back arc basins) [*Kelemen et al.*, 1995a]. In contrast, surrounding, residual peridotites preserve mineral compositions far from equilibrium with MORB [*Kelemen et al.*, 1995a]. Thus dunites

in the Oman mantle section mark conduits for focused flow of melt through the uppermost mantle in a process that preserved disequilibrium between migrating liquid and surrounding peridotite.

[6] In general, field evidence from ophiolites demonstrates that most or all dunites formed via in situ replacement due to opx dissolution and concomitant olivine precipitation during porous flow of olivine-saturated melt through opx-bearing peridotite [*Kelemen et al.*, 1995a]. Therefore some dunites may form purely as a result of reactive porous flow processes, and the presence of melt filled cracks is not required to explain them. Furthermore, *Kelemen et al.* [1997] showed that focused flow of melt in porous conduits can satisfy melt velocity constraints derived from uranium series disequilibria in MORB [*Lundstrom et al.*, 1995, 1999; *Sims et al.*, 1995; *Volpe and Goldstein*, 1993] and from the timing of volcanism due to decompression melting following deglaciation in Iceland [*Slater et al.*, 1998; M. Jull and D. McKenzie, The effect of deglaciation on mantle melting beneath Iceland, submitted to *Journal of Geophysical Research*, 1995], so that melt transport in cracks is not required by these data, either. However, some dunites show evidence for formation as porous reaction zones around cracks [e.g., *Kelemen et al.*, 1995a, Figure 2F and 2G], and in general the geologic evidence does not rule out the possibility that many dunites form in this way [*Nicolas*, 1986, 1990; *Nicolas and Jackson*, 1982; *Suhr*, 1999].

[7] Regardless of their general mode of formation it is evident that dunites mark the site of focused melt transport through the uppermost mantle in ophiolites. In this study, we characterize the geometry of dunites in ophiolites to constrain the nature of melt transport networks in the shallow mantle. In addition, we evaluate whether size/frequency and spatial distribution statistics are consistent with an origin via reactive porous flow and/or reaction zones around cracks.

2. Observations

[8] We made detailed maps of dunites in mantle exposures of the Ingalls ophiolite in the central Washington Cascades [*Miller*, 1985; *Miller and Mogk*, 1987] from aerial photomosaics of well-exposed dunites in nearly planar, subalpine, glaciated outcrops formed along a prominent joint set sloping $\sim 25^\circ$ to the south. More than 95% of the dunites, which are tabular and cylindrical in form, are oriented approximately perpendicular to these outcrop surfaces. This is demonstrated by structural data (Figure 1) and from outcrop patterns in a second set of exposures along a joint set sloping at $\sim 75^\circ$ to the north. Along these north facing outcrops, dunites form parallel-sided features, with near vertical dips, which do not intersect. Thus, on the south-facing slopes, the outcrop width of dunites is equivalent to their true width. Mapped dunites range in width from ~ 3 mm to a few meters in three outcrops, with each outcrop having an area of the order of 600 m^2. There are size cutoffs in the data set for two reasons: (1) at length scales approaching the grain size, it becomes a philosophical issue to distinguish between "dunites" and the continuous matrix of olivine within peridotites; (2) at the largest sizes, dunites are preferentially weathered compared to residual peridotites and commonly define the edges of the outcrops.

[9] Dunites in this area are hosted by residual mantle harzburgites, containing olivine + opx + spinel, with little or no cpx. Both dunites and harzburgites in this area preserve lattice preferred orientations in olivine, with a strong *a* axis lineation plunging gently to the NNW

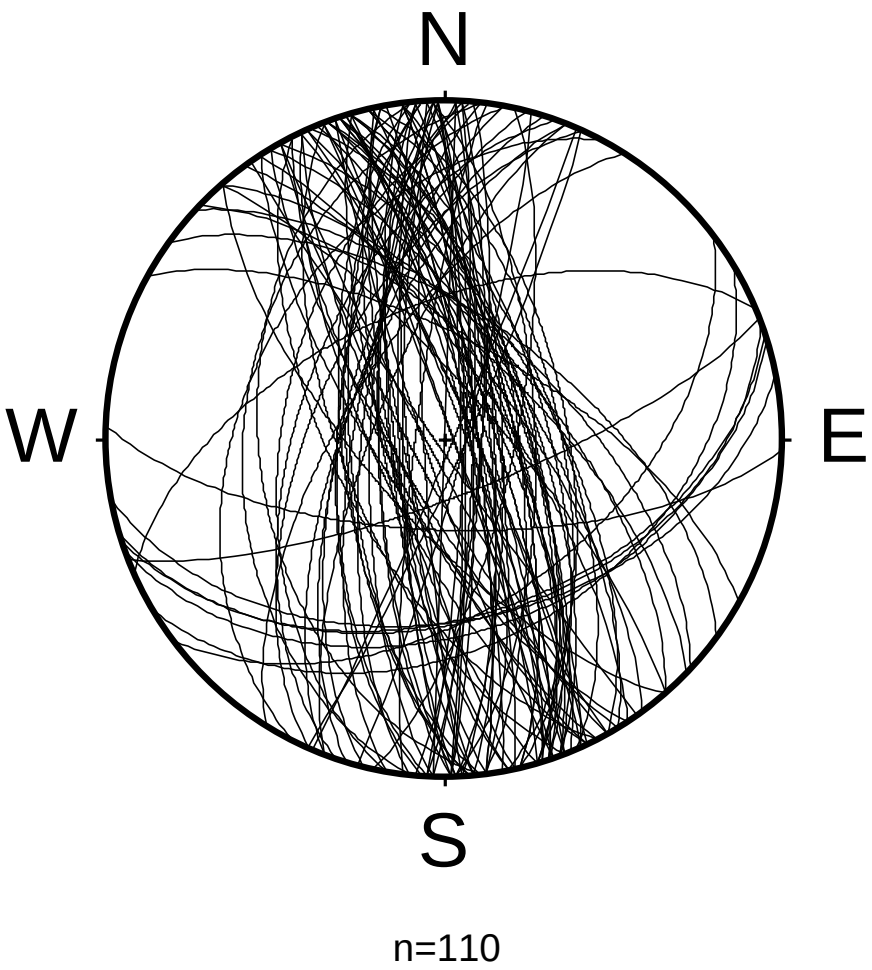

Figure 1. Lower hemisphere projection of orientation of dunites within residual mantle peridotite (harzburgite) in Bean Creek outcrops of the Ingalls ophiolite. Most dunites are approximately perpendicular to the surfaces of outcrops dipping 25°S, which were mapped for this study.

[*Miller and Mogk*, 1987]. Most tabular dunites have a NW strike, with steep dips as mentioned above. Qualitatively, the NW striking dunites form two groups, one striking ~330° and the other 350° (Figure 1). Another group, less evident on the stereonet, is seen in "Outcrop 4" (Figure 2) as a few wider, lensoid dunites, striking ~10° with steep dips. Finally, some of the widest dunites are steeply plunging cylinders, circular in the plan form of the south facing outcrop surfaces. The most prominent of these is the largest dunite in the "Ball outcrop" (Figure 2).

[10] In order to make the maps in Figure 2, we prepared outcrops by outlining the dunite/peridotite contacts with marking pens. Overlapping photographs were taken along an orthogonal grid from a helium blimp (Blimp for On-Land Oceanography, BOLO) 7 m above the outcrop, with the camera lens approximately perpendicular to the surface.

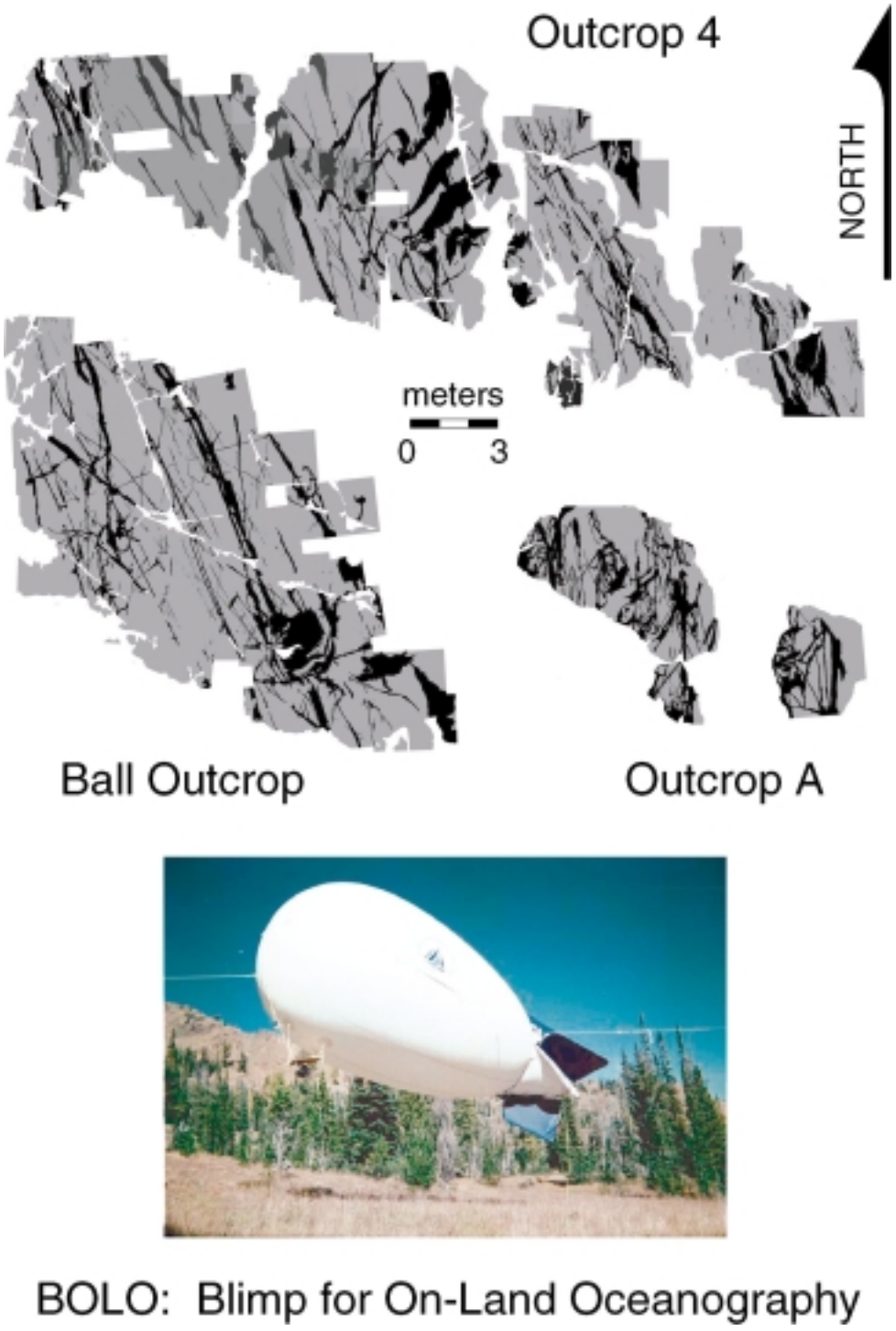

Figure 2. Photomosaic maps of three outcrops from the Bean Creek area, Ingalls ophiolite. Grey, residual mantle peridotite (harzburgite); black, dunite; white, areas with no outcrop, including eroded dunites.

Each photo frame covers ~2.5× 1.5 m. In the laboratory we reduced the photos to line drawings, scanned these drawings, and prepared digital photomosaics (Figure 2). Minimal distortion of each image, required to combine them into a mosaic, was done using Adobe Photoshop® software.

[11] Dunite widths and spacing were determined via an "intercept length" method. A grid of 100 parallel lines 1 pixel wide was superimposed at a fixed azimuth on each outcrop image; the dimensions of pixels varied from image to image, ranging from 0.0031 m for the photomosaic of the Ball outcrop to 0.0046 m for outcrop A. Lengths of line segments intersecting dunites, or intersecting harzburgites, were determined using Ultimage Pro® software. Each set of intercepts contained ~1500 measurements of dunite width or spacing. For dunite widths this process was repeated for parallel lines striking 90°, 80°, 70°, 60°, and 50°, designed to be roughly perpendicular to most of the dunites. The resulting widths were found to be relatively insensitive to the azimuth of the lines, so the intercept lengths were combined into a single data set of ~7500 measurements for each outcrop. Dunite spacing was only measured along lines with an azimuth of 70°.

[12] Dunite width statistics show a clear power law relationship between frequency per meter of intercept measurement (N_l) and intercept length (w), in which $N_l = A\, w^n$ (Figures 3A to 3D). For all three outcrops, $A \approx 0.02$ and $n \approx -3$. Dunite spacing (s), in contrast, is exponential, with $N_l = A'\, e^{B\, s}$ (Figures 3D to 3F). The fits for both width and spacing are particularly good for the Ball outcrop, for which we have the best image quality and thus the most accurate statistics for small sizes. Unlike the width/frequency statistics, however, A' and B are not consistent from outcrop to outcrop.

[13] The observation of exponential spacing/frequency statistics is complicated by a systematic relationship between spacing and dunite width. Many of the larger dunites are approximately parallel and show a preferred spacing of ~2 m. As illustrated in Figure 4, this value was quantified for a portion of the Ball outcrop using a two-dimensional correlation length routine developed by D. Smith (1998) at Woods Hole.

3. Interpretation

[14] Two simple hypotheses might explain the spatial distribution statistics of the dunites described above. (1) The dunites formed part of a coalescing network of channels, in which many small channels fed a few larger ones [e.g., *Aharonov et al.*, 1995; *Kelemen et al.*, 1995b; *Spiegelman et al.*, 2000]. (2) The dunites formed as porous reaction zones around melt-filled cracks [e.g., *Suhr*, 1999]. Both of these processes can give rise to a power law relationship between width and frequency and an exponential relationship between spacing and frequency, over the observed range of width and spacing in our data sets.

3.1. Coalescing Network Hypothesis

[15] A simple example of a coalescing fluid transport network is illustrated in Figure 5A ("Einat's Castle," from *Aharonov et al.* [1995, Figure A1]. Here pairs of small channels join to form larger ones at regular heights. At each junction the number of channels decreases by a factor of 2 and the flux per channel increases by a factor of 2, giving rise to a power law relationship between frequency of channels with a given flux N and flux per channel, Q_c, in which $N \propto Q_c^n$ with $n = -1$. These statistics apply to the entire "system" and not to any specific horizontal section through the network.

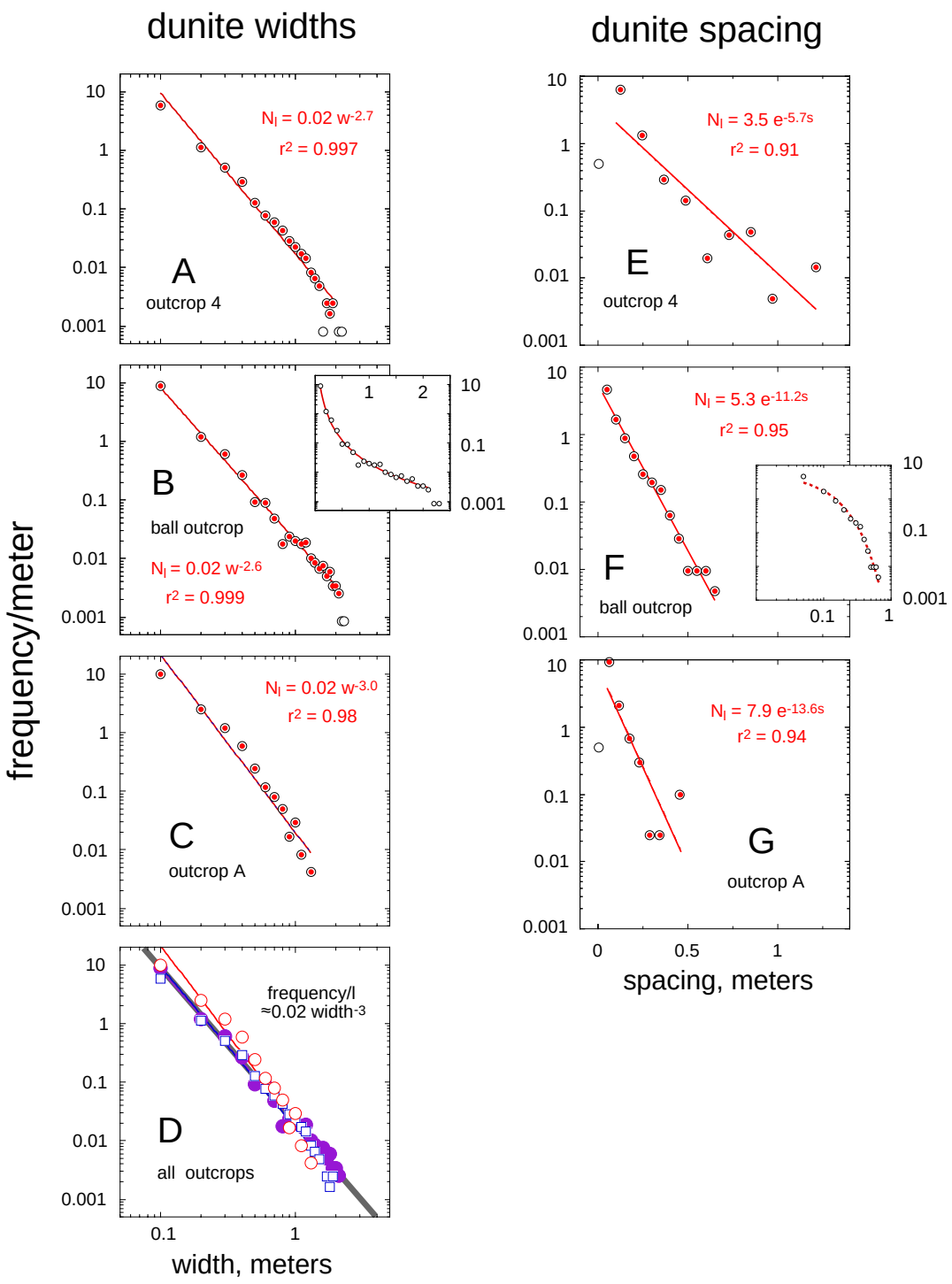
dunite widths
dunite spacing
frequency/meter
A
outcrop 4
$N_l = 0.02\ w^{-2.7}$
$r^2 = 0.997$
B
ball outcrop
$N_l = 0.02\ w^{-2.6}$
$r^2 = 0.999$
C
outcrop A
$N_l = 0.02\ w^{-3.0}$
$r^2 = 0.98$
D
all outcrops
frequency/l
≈0.02 width^{-3}
width, meters
E
outcrop 4
$N_l = 3.5\ e^{-5.7s}$
$r^2 = 0.91$
F
ball outcrop
$N_l = 5.3\ e^{-11.2s}$
$r^2 = 0.95$
G
outcrop A
$N_l = 7.9\ e^{-13.6s}$
$r^2 = 0.94$
spacing, meters

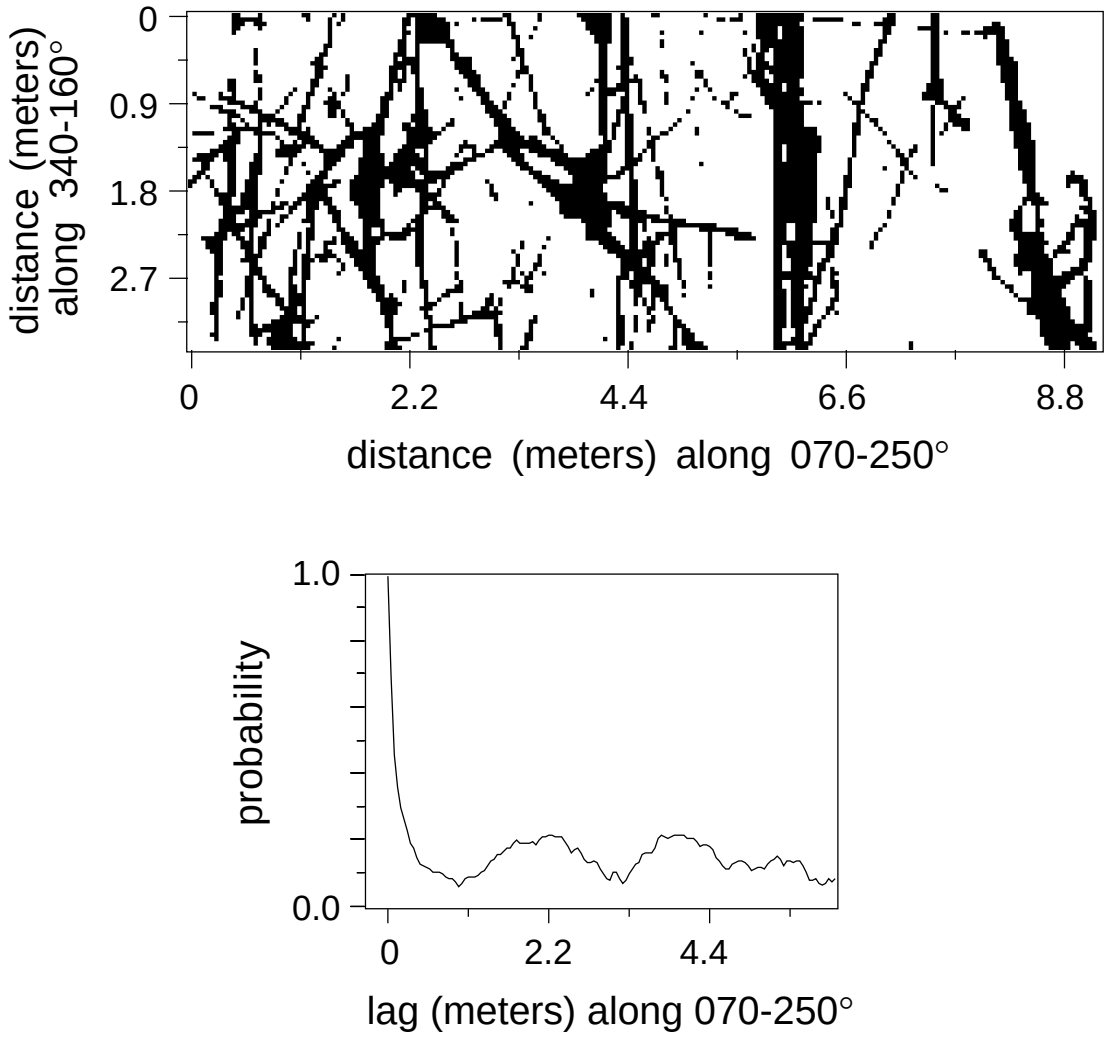

Figure 4. Lower-resolution image from the Ball outcrop (Figure 2), and results of two-dimensional autocorrelation analysis of this image. Note that for this analysis, eroded areas which we interpreted as dunites were treated as dunite outcrop areas.

[16] A channel network predicted by a numerical model of reactive porous flow, in which a solvent migrates through a partially soluble, porous medium subject to viscous compaction

Figure 3. Spatial distribution statistics for dunites from Figure 2. All data shown as open circles; smaller, solid circles indicate data used in fitting equations. (A, B, C and D) Frequency of dunite widths, determined using an intercept method as described in the text. These data are well fit using a power law relationship. The inset in Figure 3B shows the same data and fit, but here on a linear-log plot, illustrating that the size/frequency data are not well described by an exponential relationship. Figure 3D is a compilation of data from all three outcrops. Wide grey line in Figure 3D has a power law slope of −3.0. (E, F, and G) Frequency of spacing between dunites. These data are well fit using an exponential relationship. The inset in Figure 3F shows the same data and fit, but here on a log-log plot, illustrating that the spacing/frequency data are not well fit using a power law relationship.

[*Spiegelman et al.*, 2000], is shown in Figure 5B. Because more than 95% of the porous flow occurs within channels, and similar-sized channels undergo pairwise coalescence at regular intervals, the resulting channel geometry is remarkably similar to that in Figure 5A, with $N_l \propto Q_c^{-0.98}$ measured using an intercept technique. Determining intercept lengths of channels, marked by a decrease in the soluble phase concentration, gives $N_l \propto w^n$, where the value of n depends on the concentration threshold used. Finally, one can discern an exponential relation between spacing and N_l in the model results. Again, these statistics have been derived for the entire vertical channel system and may not be present within any horizontal section through the model results.

[17] A much more complicated, two-dimensional network is shown in Figure 5C. Here coalescence is mainly pairwise, as above, but very small channels sometimes join very large ones, termed "side branching" [*Tokunaga*, 1978; *Turcotte*, 1997]. Despite the complication of side branching, in coalescing channel networks in which $Q_c \propto w^n$ and $N_l \propto Q_c^{-1}$, it is found that $N_l \propto w^n$. Two examples of coalescing networks with abundant side branching are arterial and bronchial networks in animals. Our analysis of data on bronchial tubes the human lung [*Wilson*, 1967] and cat arteries [*Fung*, 1984] gives $n = -2.7$ and $n = -2.5$, respectively, with correlation coefficient r^2 greater than 0.996 in both cases. Intercept measurements on the network in Figure 5C, using the same methods as those used to produce the dunite statistics in Figure 3, give $n = -3.5$. Strikingly, for some large networks with side branching the spacing between channels is closely approximated by an exponential function. For example, in Figure 5C, $N_l \propto e^{-0.07s}$. In the context of interpreting our data on dunite distribution, note that in these networks with side branching, horizontal sections would also show power law width/frequency statistics, although coalescence would not be visible in such sections.

[18] In the case of the Ingalls peridotite the dunite "network" is clearly three dimensional, but the dunites themselves are generally tabular. Thus the dunites can be approximated as parallel, tabular features with infinite length. In the context of this coalescing network hypothesis we can infer that they coalesce upward, in a network whose paleovertical cross section might resemble Figure 5C. We infer that we have mapped a paleohorizontal plane in the Ingalls outcrops since the outcrop surface is perpendicular to 95% of the dunites. As for the network in Figure 5C, a paleohorizontal plane through a similar dunite network should exhibit power law width/frequency statistics but should rarely exhibit coalescence.

[19] Figure 5 illustrates that our data on width/frequency of dunite veins are consistent with the hypothesis that they formed a coalescing network of porous, tabular channels. In tabular, porous channels, $Q_c = wu\phi$, where u is melt velocity and ϕ is porosity. In a coalescing network that conserves flux, in which $N \propto Q_c^{-1}$, and $N \propto w^{-3}$ (as in our results), then $Q_c \propto w^3$. During flow of melt in a porous channel, Darcy flux, $u\phi$, is proportional to permeability, which in turn varies with ϕ^m, where m is 2 to 3. In this case, with $Q_c = wu\phi \propto w^3$, it follows that $\phi \propto w^{2/m}$. Thus our results suggest that porosity increased with increasing width of dunite channels.

[20] Increasing porosity with width may not continue within ever larger dunites. For example, a reasonable minimum porosity within dunites is $\sim$0.001. This is based on the observation that many dunites do not include detectable "trapped liquid" in the form of

Einat's Castle

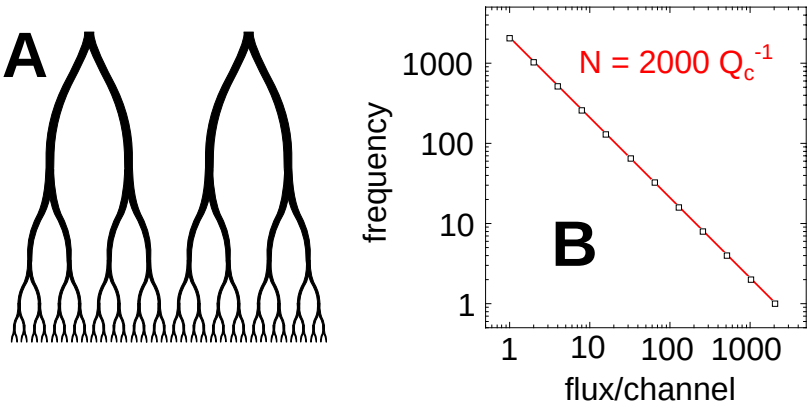

numerical results

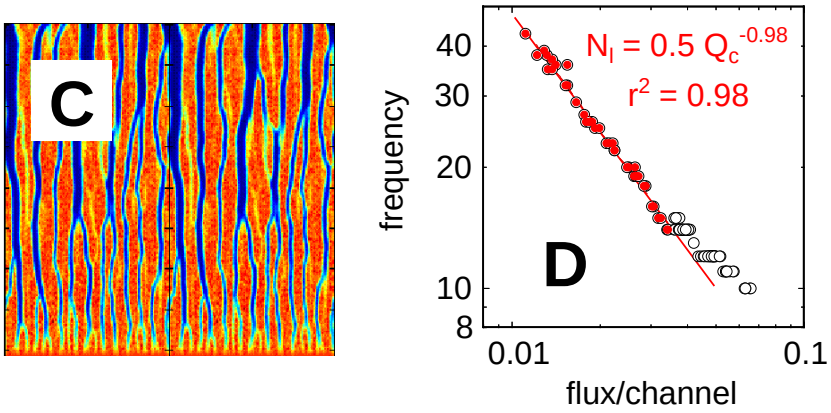

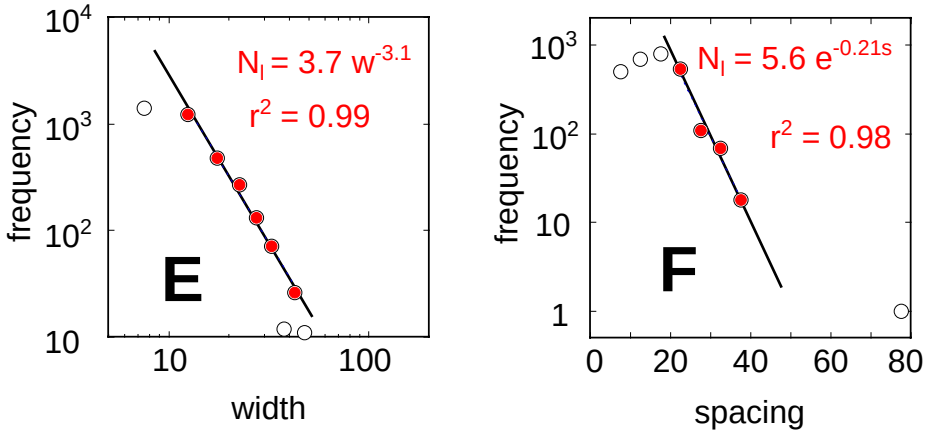

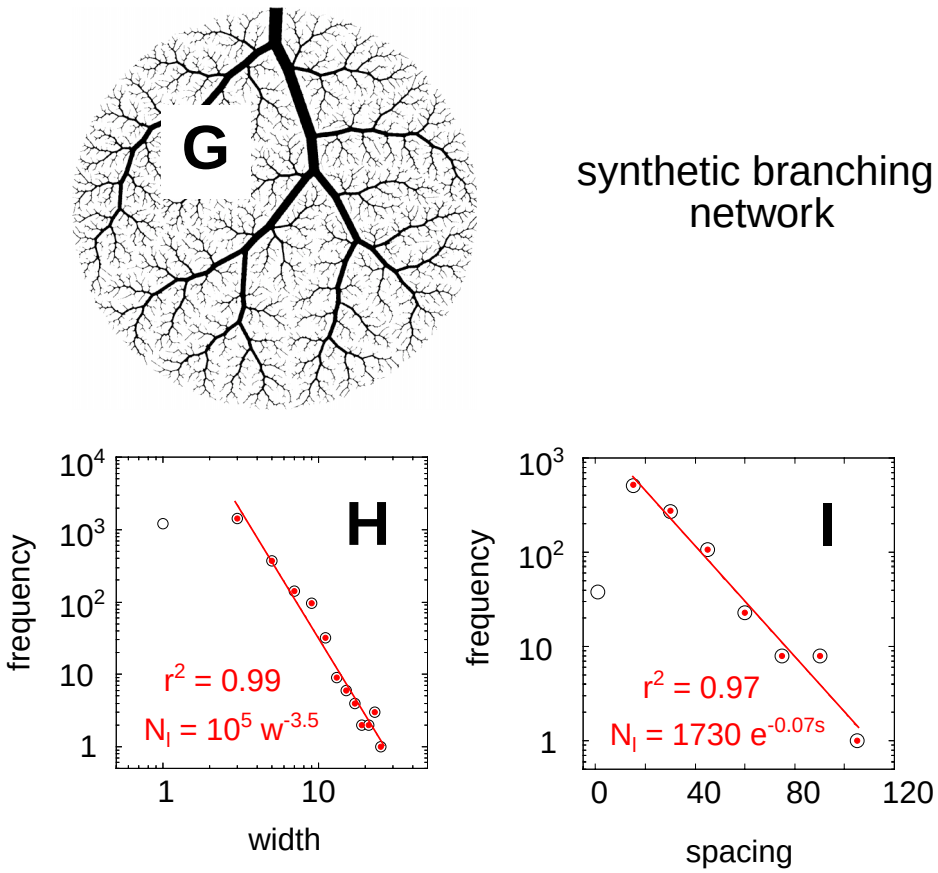

Figure 5. Coalescing channel networks with spatial distribution statistics similar to those of the dunites in Figure 2. All data shown as open circles; smaller, solid circles indicate data used in fitting equations. (A and B) "Einat's Castle" from Figure A1 of *Aharonov et al.* [1995]. (C, D, E, and F) Results of numerical modeling of the reactive infiltration instability [*Spiegelman et al.*, 2000], in a two-dimensional system undergoing porous flow and viscous compaction, with a fixed flux of solvent through the bottom boundary, a free top boundary, wrap-around side boundaries (image is repeated once). Figure 5C is a map of the concentration of the soluble phase after some time, from 0.25 (red) to 0.00 (black), showing elongate channels, coalescing and widening upward. Flux/channel (Figure 5D) and channel width (Figure 5E) both show a power law relationship with frequency, whereas frequency/spacing (Figure 5F) can be fit with an exponential function. (G, H, and I) Synthetic, two-dimensional "arterial" network from Figure 2D of *Schreiner et al.* [1997]. Again, frequency/channel width shows a power law relationship (Figure 5H), whereas frequency/spacing is exponential (Figure 5I).

pyroxene and plagioclase crystals, and the estimate that we could detect these phases if they formed more than 0.1% of the rock. If we assume that the porosity in 0.01 m dunites was 0.001, and m = 2, then one would infer from the relationship discussed in the previous paragraph that porosity in dunites wider than 10 m would be greater than 1, which is not possible. However, for porosity in 0.01-m channels of 0.001 and m = 3, then the porosity in dunites 10 m wide would be ~0.1, which may be reasonable. Alternatively, there may be a maximum porosity within channels, which is reached when the increasing rate of viscous compaction (due to the exponential decrease in bulk viscosity as

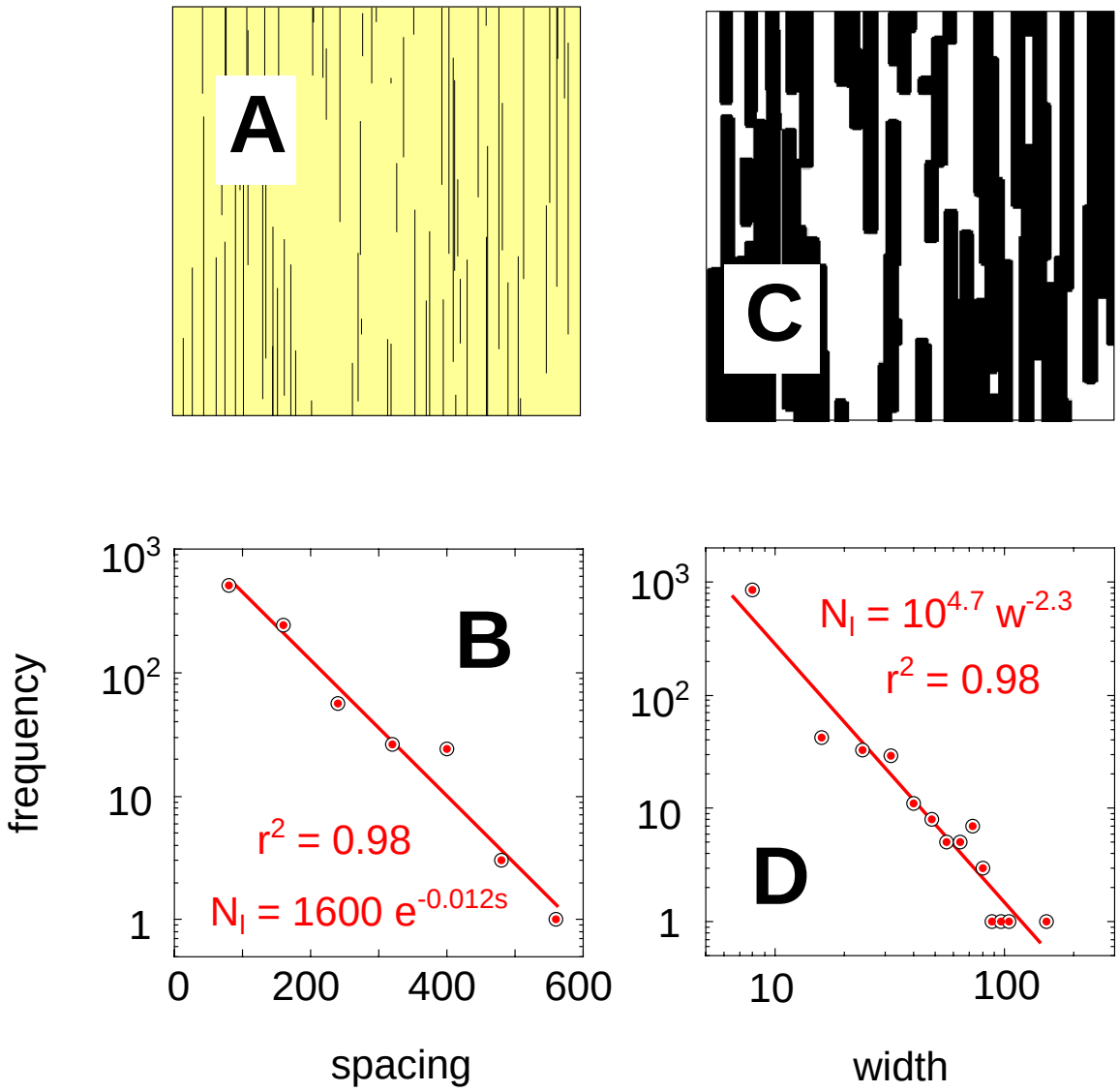

Figure 6. Results of a simple model of reaction zones around parallel cracks. (A and B) Randomly spaced, parallel cracks, and their spacing statistics; (C) reaction zone distribution after 15× widening of initial, 1 pixel wide "reaction zones"; (D) size/frequency statistics when reaction zones occupy 80% of a model space larger than Figure 6C.

a function of porosity in partially molten mantle rocks [*Hirth and Kohlstedt*, 1995a, 1995b; *Kelemen et al.*, 1997]) becomes equal to the rate of unstable formation of pore space due to reactive porous flow of ascending melt. Width/frequency measurements for very large dunites, for example, in the Oman ophiolite, may help provide constraints on this question.

3.2. Reaction Zones Around Cracks

[21] If dunites form as porous reaction zones around melt-filled cracks and cracks closed

without a trace, only dunite reaction zones would remain in the outcrops. To model the implications of this hypothesis, we simulated growth of reaction zones around a random distribution of infinitesimally thin, parallel cracks, assuming that dunites grow simultaneously and at the same rate around each crack. In a plane perpendicular to the cracks the initial crack distribution gives rise to an exponential relationship between frequency and crack spacing, with $N_l \propto e^{-0.012s}$ (Figures 6A and 6B). As reaction zones widen, individual dunites around adjacent cracks merge to form larger dunites. In general, these events involve pairwise merging. Thus, between the inception of reaction zone growth and the time at which reaction zones fill all of the space, there is an approximate power law relationship between dunite width and frequency (Figures 6C and 6D). We simulated the same process for formation of reaction zones using a natural crack distribution [*Segall and Pollard*, 1983]. Although natural cracks are thought to exhibit nonrandom clustering [*Renshaw and Pollard*, 1994], we found that they have an approximately exponential spacing/frequency relationship and that merging of reaction zones produced a power law size/frequency relationship at intermediate times, as for the simpler example illustrated in Figures 6C and 6D.

[22] We prefer hypothesis 1 as an explanation for the spatial statistics of dunites in the Ingalls peridotite for several reasons. First, a power law relationship between width and frequency spanning 1 order of magnitude in width, resulting from growth of reaction zones as in hypothesis 2, arises only when the largest dunites have formed by the random merging of at least 10, adjacent reaction zones. For either randomly distributed cracks, or natural, clustered arrays of cracks, power law size/frequency relations spanning an order of magnitude in size are only attained when the reaction zones fill more than 75% of the area in a plane perpendicular to the cracks. (For the result in Figure 6D the reaction zones occupy 80% of the area). In contrast, dunites comprise only 23% of our study area in the Ingalls ophiolite.

[23] Second, although many of the smaller dunites in the Ingalls outcrops are highly elongate, with shapes that qualitatively resemble cracks, the largest dunites are those with aspect ratios (length/width) close to 1. In contrast, melt-filled cracks preserved as dikes have aspect ratios $\sim$100 or (commonly) more [*Delaney and Gartner*, 1997], in accord with theory [e.g., *Broek*, 1978; *Pollard and Segall*, 1987]. Hypothesis 2 relates Ingalls dunites to reaction zones around cracks, rather than to cracks themselves. For diffusive growth of reaction zones around a melt-filled crack the crack can be viewed as an infinite reservoir of melt with constant composition. In this case, the rate of growth of the reaction zones is independent of the width of the crack. However, one might infer that larger cracks are melt filled for a longer time. It seems unlikely that the cracks with the widest reaction zones would be those with the smallest length and width.

[24] Third, constant growth of reaction zones around random cracks cannot explain why the larger reaction zones would have a preferred wavelength, as seen in our data, particularly in the Ball outcrop (Figure 2).

[25] Fourth, we find that the maximum width of dunite veins in the Oman ophiolite mantle section is $\sim$100 m (Table 1), and the minimum width is $\sim$0.01 m. Given the assumptions of hypothesis 2, all of these dunites have been growing at the same rate for the same amount of time. In this case, explaining this range in sizes would require merging of more than 10,000 reaction zones

Table 1. Measured Widths of Large Dunites in the Mantle Section of the Oman Ophiolite[a]

Locality	Minimum Thickness, m	Universal Transverse Mercator Location
Hilti massif, near basal thrust	66.5	2647546 N, 0429502 E
Hilti massif, near basal thrust	21	2658672 N, 0429390 E
Muscat area, Dog Peak	90	approx 2612300 N, 0661600 E
Wadi Tayin massif, Batin north, #1	69.4, 94.8	2540674 N, 0672630 E
Wadi Tayin massif, Batin north, #2	32.8	as above
Haylayn massif, Wadi Mabrah	~50	2597965 N, 0493841 E
Sumail massif, Wadi Lufti #1	51	2571822 N, 0633216 E
Sumail massif, Wadi Lufti #2	16.7	as above
Sumail massif, Wadi Lufti #3	33.7	as above
Sumail massif, Wadi Lufti #4a	34	as above
Sumail massif, Wadi Lufti #4b	51, 42	as above

[a]All widths were determined by Kelemen and Braun via chain and compass mapping of large tabular dunites that are completely surrounded by residual, mantle harzburgite, more than 1 km structurally below the crust/mantle transition zone. The best exposed, large dunites we have mapped are (1) in the area between Muscat and Muttrah, but not in laterally continuous parts of the same mantle massif to the south, between Al Bustayn and Ruwi (our ongoing work), (2) in the eastern Wadi Tayin massif several kilometers structurally below the MTZ, but not in the western half of the massif at the same depth below the MTZ [*Hopson et al.*, 1981], and (3) near the base of the Hilti massif, ~5 km structurally below the MTZ, but not at shallower depths below the MTZ [*Bishimetal Exploration*, 1987].

to produce the largest dunites. This seems highly improbable.

4. Discussion

[26] We prefer the hypothesis in which the Ingalls dunites formed a coalescing channel network, in which flux was conserved downstream, and channel width was proportional to flux. Such a channel network could be produced as a result of the reactive infiltration instability [*Chadam et al.*, 1986; *Ortoleva et al.*, 1987]. According to this theory, diffuse flow of a solvent through a soluble porous matrix is unstable. Infinitesimal variations in permeability give rise to higher fluid flux in some areas, which in turn leads to more dissolution, raising the permeability, in a feedback mechanism that gives rise to dissolution channels that grow exponentially. At longer times the fastest growing channels entrain more of the total flux, starving their neighbors, leading to a decreasing number of more widely spaced features [*Kelemen et al.*, 1995b]. As discussed by *Aharonov et al.* [1995], scaling relationships based on a linear stability analysis suggest that unstable formation of dissolution channels in viscously compacting porous media could give rise to a coalescing channel network (Figure 5A).

[27] The self-similar, "fractal" branching of this hypothetical network is similar to that proposed by *Hart* [1993] although, unlike Hart, Aharonov et al. envisioned a network of porous conduits, not open, melt-filled cylinders, and provided a physical explanation of how such a network might arise in the Earth's mantle. The Aharonov et al. prediction is supported by results of numerical modeling by *Spiegelman et al.* [2000] as illustrated in Figure 5B. In the numerical model a solvent enters the bottom boundary of the model, and rises through a partially soluble, viscously compacting porous medium. Solubility is inversely related to pressure. The solvent is initially in equilibrium with the porous matrix, but must dissolve solids to maintain equilibrium as it rises, approximating the phase relations of melt rising through the upper mantle along an adiabatic geotherm [*Asimow and Stolper*, 1999; *Kelemen et al.*, 1995b]. Eventually, dissolution of pyroxene from residual peridotite within such channels would give rise to dunites. Thus the formation of a coales-

cing network of dunite veins is a predictable consequence of reactive porous flow of melt in the adiabatically convecting upper mantle.

[28] While our data show an exponential spacing/frequency relationship, results of numerical modeling of the reactive infiltration instability show a regular spacing between channels, increasing downstream (Figure 5B). However, in numerical models completed to date, most of the "melt" enters the system from below, and additional melt is generated only by dissolution reactions. In contrast, in the adiabatically upwelling mantle beneath a spreading ridge, melt would be generated internally owing to adiabatic decompression in addition to the flux of melt from below and to melt generated by dissolution reactions. We suggest that this process must lead to formation of a variety of channel sizes at every depth, similar to the channel network in Figure 5C. Larger channels, originating at greater depth, might show regular spacing as in Figure 5A and 5B, whereas the smaller channels might be more randomly distributed giving rise to an exponential spacing/frequency distribution.

[29] Although our data are generally consistent with an origin for dunites via reactive porous flow, we cannot rule out a role for melt-filled fractures in forming the Ingalls dunites. Note that hypothesis 2, as formulated above, is very simple. More complex scenarios can easily be envisioned. For example, perhaps dunites originated as reaction zones around cracks but then became important conduits for porous melt transport. Then the reactive infiltration instability and similar feedback mechanisms could begin to play a role, enlarging a few dunites at the expense of many smaller ones. Such a scenario may have been envisioned by *Suhr* [1999]. In such a process the initial cracks play the same role that initial, infinitesimal permeability perturbations play in the reactive infiltration instability that was described above, providing initial sites that nucleate the unstable growth of porous dissolution channels. Thus, in such hybrid models, cracks do not play a fundamental physical role in developing the power law size frequency relationships that are seen in our data.

[30] A crucial difference between dissolution channels in simple models and observed dunite veins is their three-dimensional morphology. Three-dimensional numerical models of dissolution channel formation via the reactive infiltration instability in rigid, soluble porous media show that dissolution channels are roughly cylindrical [*Aharonov et al.*, 1997], whereas most dunites in the mantle section of ophiolites are tabular features. These differences may arise because the dunites form by some mechanism other than the reactive infiltration instability or because the dunites form as a result of reactive porous flow but in rocks in which the permeability is strongly anisotropic. Anisotropic permeability might arise if melt topology is controlled by grain shape and/or lattice preferred orientation of olivine [*Phipps Morgan*, 1987], non-hydrostatic stress conditions [*Daines and Kohlstedt*, 1997; *Zimmerman et al.*, 1999], and/or from the initial presence of cracks [*Suhr*, 1999]. The apparent existence of two sets of preferred orientations for NW striking, narrow, tabular dunites (Figure 1), with planes $\sim 20^\circ$ apart, is consistent with observations of anisotropic melt pore shapes due to nonhydrostatic stress [*Daines and Kohlstedt*, 1997; *Zimmerman et al.*, 1999]. Regardless of the initial reason for formation of tabular dunites, melt flow in tabular channels might focus into cylindrical channels over time, as is predicted for flow of lava through tabular dikes (e.g., K. R. Helfrich, Thermo-viscous fingering of flow in a thin gap: Application to magma emplacement, submitted to *Journal of Fluid Mechanics*, 1995) thus providing a possible explanation for the presence of "cylindrical"

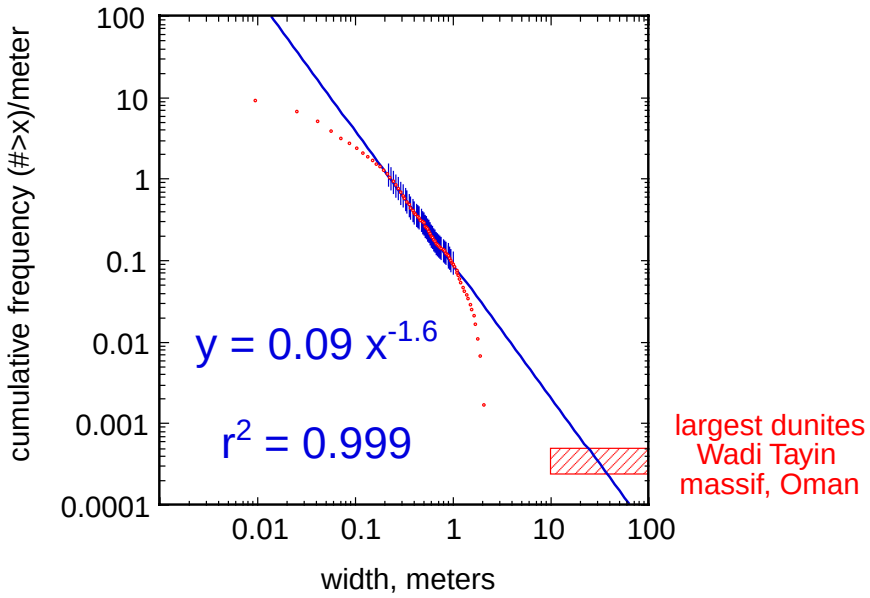

Figure 7. Dunite width in Ball outcrop (Figure 2) versus cumulative frequency (number of observations with width greater than x). Data for dunite width greater than 0.2 m and less than 1 m, where sampling density is high, were fit to derive a power law relationship, which was then extrapolated to the sizes of the largest dunites in the mantle section of the Oman ophiolite. The small-scale data from the Ingalls ophiolite are roughly consistent with the frequency of large dunites in Oman.

dunite veins, with cross-sectional aspect ratios near 1, in our Ingalls data.

[31] Size/frequency and spatial distribution statistics on dunites in ophiolites might be used to estimate the range of sizes and the spatial distribution for dunite conduits that are present in the entire melting region beneath oceanic spreading ridges. In a preliminary comparison of our Ingalls data set from the Ball outcrop to dunite distribution in one of the massifs in the Oman ophiolite (Figure 7), we have used a cumulative histogram because this facilitates comparison of data sets that have intrinsically different size cutoffs due to different observation methods [*Turcotte*, 1997]. A drawback of this method is that power law behavior is only exhibited over a limited size range due to observational cutoffs. Thus, determining a power law slope is somewhat qualitative. We fit the dunite width data for all sizes between 0.2 and 1 m. For the mantle section of the Wadi Tayin massif of the Oman ophiolite, an intercept method was used, together with field observations on the true width of large, tabular dunites. This yields $\sim$10 dunites with true widths of 10 to 100 m along 40 km of intercept measurements, a frequency of 2.5×10^{-4} m^{-1}. Most of the large dunites are concentrated in the eastern half of the Wadi Tayin mantle section. Thus intercept measurements on the eastern half would yield $\sim 5\times 10^{-4}$ m^{-1}. Our data from the Ingalls peridotite are seen to be very approximately consistent with the distribution of large dunites in the Wadi Tayin massif (Figure 7), suggesting that there may be a single size/frequency relationship for the entire range of mantle dunite sizes. However, our preliminary, detailed measurements of size/frequency relationships for dunites in Oman show a much lower slope (M. Braun et al., personal communication, 2000).

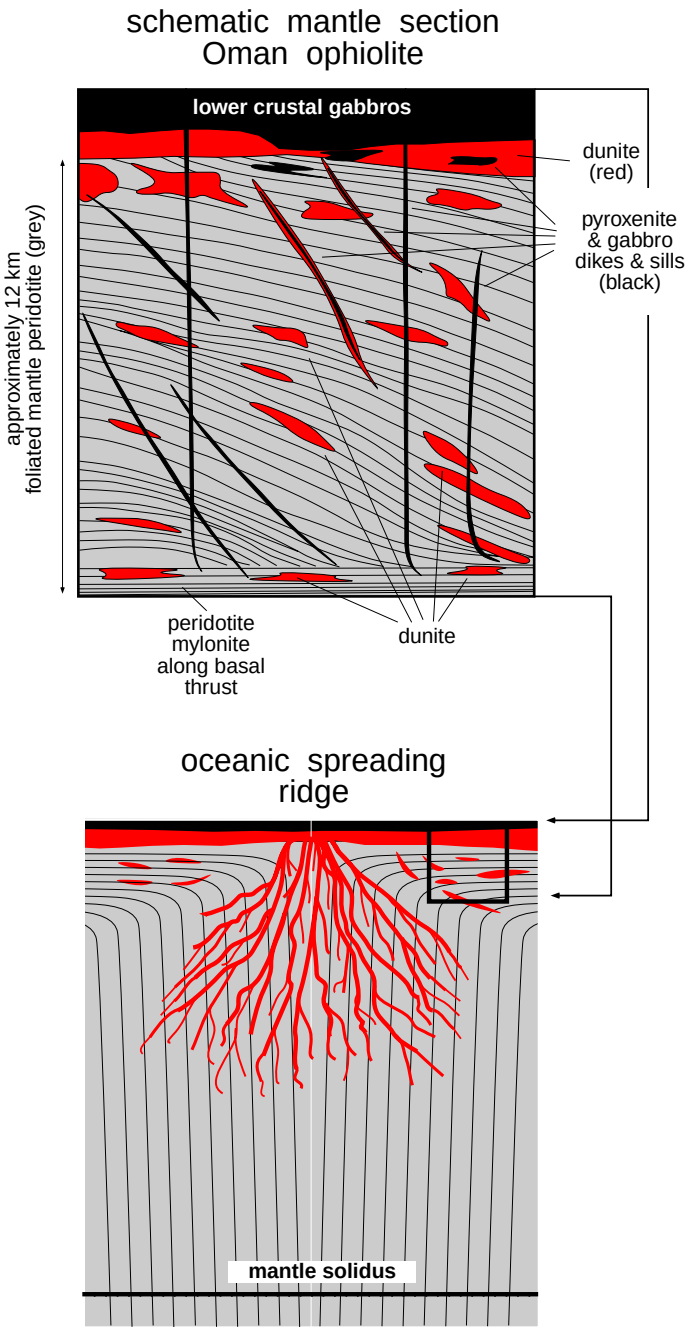
schematic mantle section
Oman ophiolite
lower crustal gabbros
dunite
(red)
pyroxenite
& gabbro
dikes & sills
(black)
approximately 12 km
foliated mantle peridotite (grey)
peridotite
mylonite
along basal
thrust
dunite
oceanic spreading
ridge
mantle solidus

[32] All of our width/frequency statistics certainly need to be refined before they are used for extrapolation. As mentioned in the previous paragraph, there is clear clustering of dunites in both the Ingalls and Oman ophiolites. In the Ingalls ophiolite we chose the Bean Creek area because of its abundant dunites. Reconnaissance in the area around Ingalls Lake revealed that dunites were comparatively rare, perhaps 5% of a $\sim$100,000 m^2 area. Reconnaissance around Scatter Mountain revealed an outcrop area of $\sim$100,000 m^2 with no dunites at all. Similarly, in the Oman ophiolite there are areas of abundant dunite veins and other areas with very few. If our measurements included areas with low dunite density, this would obviously lower the frequency/meter for dunites of a given width. However, it is likely that incorporating data from these areas would not significantly affect the slope of the width/frequency histograms.

[33] The exponential relationship between dunite spacing and frequency almost certainly cannot be extrapolated to areas with few dunites. For example, there are certainly 10-m sections of mantle peridotite in the Wadi Tayin massif of the Oman ophiolite with no dunites. Along the 40 km of intercept length used for Figure 7 we are certain that at least one such section would be encountered, so the minimum frequency for a 10-m spacing would be 2.5×10^{-5} m^{-1}. In contrast, the spacing/frequency relationship for the Ball outcrop in Figure 3F would predict a frequency of $\sim 10^{-48}$ m^{-1} for 10-m spacing.

[34] We do not yet understand the systematics of dunite clustering. Nicolas and coworkers have emphasized that dunites are common near the crust/mantle transition zone (MTZ [e.g., *Jousselin et al.*, 1998]). However, there are also abundant large dunites (10 to 100 m in width) many kilometers below the MTZ, with a heterogeneous, clustered lateral and vertical distribution. We have measured the widths of numerous subparallel dunites with widths of 10 to 100 m in several places (Table 1) that are several kilometers below the MTZ in the mantle section.

[35] We now return to the two constraints on melt extraction beneath mid-ocean ridges outlined in the introduction. Previous work [e.g., *Bishimetal Exploration*, 1987; *Hopson et al.*, 1981], combined with the width/frequency data and observed sizes of dunites presented here, shows that tabular dunite veins more than 1 m wide are common in ophiolite mantle sections and thus can satisfy the requirement for chemically isolated transport of melt through the shallow mantle. Our width/frequency data suggest that dunites may have been part of a coalescing channel network. Our favored hypothesis is that such a coalescing network arose spontaneously as a consequence of unstable formation of dissolution channels. If so, this process may be important in producing coalescence from the $\sim$100 km wide region of partial melting in the mantle to the $\sim$5 km wide zone of igneous crustal formation beneath oceanic spreading ridges.

Figure 8. Summary cartoon from Figure 1 of *Kelemen et al.* [1995a] showing general contact relationships of large dunites in the mantle section of the Oman ophiolite and inferred coalescing network of porous dunite channels in the adiabatically upwelling mantle beneath a fast-spreading mid-ocean ridge. Note that the network shown here resembles a bush, with many branches coalescing at the base of the lithosphere beneath the ridge, whereas that published previously [*Kelemen et al.*, 1995a] was a tree-like structure with branches entering a single, central conduit. Also, the network shown here extends for 30 to 50 km downward into the melting region in the mantle. These changes reflect our improved understanding of channel networks and of constraints from ophiolites and mid-ocean ridges. Reprinted with permission (http://www.nature.com).

[36] In conclusion, our data for dunite veins in the Ingalls peridotite in the central Washington Cascades show a power law size/frequency relationship in which frequency/meter $\propto$ width^{-3}, over a width interval from $\sim$0.1 to 2 m, and an exponential spacing relationship in which log(frequency/m) $\propto$ spacing. There may be several ways to generate such spatial relationships, but we favor the hypothesis that the dunites represent a coalescing melt transport network, in which flux from many small veins feeds a few large ones, and flow is ultimately focused to a narrow region beneath oceanic spreading ridges (Figure 8). This result is broadly consistent with the hypothesis that mantle melt extraction may occur within a fractal branching network [*Hart*, 1993] and with recent analytical and numerical results on formation of dissolution channels via flow of a solvent through a partially soluble, compacting porous medium [*Aharonov et al.*, 1995; *Kelemen et al.*, 1995b; *Spiegelman et al.*, 2000]. We are intrigued by the possibility that such networks may arise spontaneously in nature, in this case as a result of reactive porous flow where disequilibrium arises from the release of gravitational potential energy during ascent of melt.

Acknowledgments

[37] This research was supported by a Mellon Independent Study Award from the Woods Hole Oceanographic Institution to Hirth and Kelemen, and by NSF research grants EAR-9418228, and OCE-9416166. We thank Bob Miller for directing us to the best outcrops in the Ingalls peridotite. Henry Dick and Carlos Garrido nobly struggled with the Giant Tripod, a precursor to BOLO. Rachel Cox, Sara Kelemen, Scott Veirs, Carlos Garrido, and Linda Angeloni helped prepare outcrops and steer BOLO on the breezy slopes of the Bean Creek cirque. Carlos Garrido's dedication to this effort almost cost him his life; his rescue was facilitated by a gang of old friends from Seattle. Scott volunteered to replace Carlos on two hours notice, leaving Seattle at midnight and arriving in camp at 4:00 AM. Linda also provided crucial assistance in measuring dunite widths in Oman (Table 1). Marc Spiegelman provided unpublished results of modeling (Figure 5C). Rick O'Connell, Guenter Suhr, and Marc Spiegelman provided very helpful reviews.

References

Aharonov, E., J. A. Whitehead, P. B. Kelemen, and M. Spiegelman, Channeling instability of upwelling melt in the mantle, *J. Geophys. Res.*, *100*, 20,433–20,450, 1995.

Aharonov, E., M. Spiegelman, and P. Kelemen, Three-dimensional flow and reaction in porous media: Implications for the Earth's mantle and sedimentary basins, *J. Geophys. Res.*, *102*, 14,821–14,833, 1997.

Asimow, P. D., and E. M. Stolper, Steady-state mantle-melt interactions in one dimension, I, Equilibrium transport and melt focusing, *J. Petrol.*, *40*, 475–494, 1999.

Bishimetal Exploration, L., *Al Wasit Geological Map, Geol. Surv. Oman, Oman Ministry of Petrol. and Minerals*, 1987.

Bottinga, Y., and C. J. Allegre, Thermal aspects of sea-floor spreading and the nature of the oceanic crust, *Tectonophysics*, *18*, 1–17, 1973.

Brearley, M., and C. M. Scarfe, Dissolution rates of upper mantle minerals in an alkali basalt melt at high pressure: An experimental study and implications for ultramafic xenolith survival, *J. Petrol.*, *27*, 1157–1182, 1986.

Broek, D., *Elementary Engineering Fracture Mechanics*, 437 pp., Sijthoff and Nordhoff, Netherlands, 1978.

Buck, W. R., and W. Su, Focused mantle upwelling below mid-ocean ridges due to feedback between viscosity and melting, *Geophys. Res. Lett.*, *16*, 641–644, 1989.

Chadam, J., D. Hoff, E. Merino, P. Ortoleva, and A. Sen, Reactive infiltration instabilities, *J. Appl. Math.*, *36*, 207–221, 1986.

Daines, M. J., and D. L. Kohlstedt, Influence of deformation on melt topology in peridotites, *J. Geophys. Res.*, *102*, 10,257–10,271, 1997.

Delaney, P. T., and A. E. Gartner, Physical processes of shallow mafic dike emplacement near the San Rafael Swell, Utah, *Geol. Soc. Am. Bull.*, *109*, 1177–1192, 1997.

Forsyth, D., D. S. Scheirer, S. C. Webb, L. M. Dorman, J. A. Orcutt, A. J. Harding, D. K. Blackman, J. Phipps Morgan, R. S. Detrick, Y. Shen, C. J. Wolfe, J. P. Canales, D. R. Toomey, A. F. Sheehan, S. C. Solomon, and W. S. D. Wilcock, Imaging the deep seismic structure beneath a mid-ocean ridge: The MELT Experiment, *Science*, *280*, 1215–1218, 1998.

Fung, Y. C., *Biodynamics*, 404 pp., Springer-Verlag, New York, 1984.

Hart, S. R., Equilibrium during mantle melting: A fractal tree model, *Proc. Natl. Acad. Sci.*, *90*, 11,914–11,918, 1993.

Hirth, G., and D. L. Kohlstedt, Experimental constraints on the dynamics of the partially molten upper mantle, 2, Deformation in the dislocation creep regime, *J. Geophys. Res.*, *100*, 15,441–15,449, 1995a.

Hirth, G., and D. L. Kohlstedt, Experimental constraints on the dynamics of the partially molten upper mantle: Deformation in the diffusion creep regime, *J. Geophys. Res.*, *100*, 1981–2001, 1995b.

Hopson, C. A., R. G. Coleman, R. T. Gregory, J. S. Pallister, and E. H. Bailey, Geologic section through the Samail Ophiolite and associated rocks along a Muscat-Ibra Transect, Southeastern Oman Mountains, *J. Geophys. Res.*, *86*, 2527–2544, 1981.

Johnson, K. T. M., H. J. B. Dick, and N. Shimizu, Melting in the oceanic upper mantle: An ion microprobe study of diopsides in abyssal peridotites, *J. Geophys. Res.*, *95*, 2661–2678, 1990.

Jousselin, D., A. Nicolas, and F. Boudier, Detailed mapping of a mantle diapir below a paleo-spreading center in the Oman Ophiolite, *J. Geophys. Res.*, *103*, 18,153–18,170, 1998.

Kelemen, P. B., G. Hirth, N. Shimizu, M. Spiegelman, and H. J. B. Dick, A review of melt migration processes in the asthenospheric mantle beneath oceanic spreading centers, *Philos. Trans. R. Soc. London, Ser. A*, *355*, 283–318, 1997.

Kelemen, P. B., N. Shimizu, and V. J. M. Salters, Extraction of mid-ocean-ridge basalt from the upwelling mantle by focused flow of melt in dunite channels, *Nature*, *375*, 747–753, 1995a.

Kelemen, P. B., J. A. Whitehead, E. Aharonov, and K. A. Jordahl, Experiments on flow focusing in soluble porous media, with applications to melt extraction from the mantle, *J. Geophys. Res.*, *100*, 475–496, 1995b.

Kuo, L.-C., and R. J. Kirkpatrick, Dissolution of mafic minerals and its implications for the ascent velocities of peridotite-bearing basaltic magmas, *J. Geol.*, *93*, 691–700, 1985a.

Kuo, L.-C., and R. J. Kirkpatrick, Kinetics of crystal dissolution in the system diopside-forsterite-silica, *Am. J. Sci.*, *285*, 51–90, 1985b.

Langseth, M., X. LePichon, and M. Ewing, Crustal structure of the mid-ocean ridges, 5, Heat flow through the Atlantic Ocean floor and convection currents, *J. Geophys. Res.*, *71*, 5321–5355, 1966.

Lundstrom, C. C., J. Gill, Q. Williams, and M. R. Perfit, Mantle melting and basalt extraction by equilibrium porous flow, *Science*, *270*, 1958–1961, 1995.

Lundstrom, C. C., D. E. Sampson, M. R. Perfit, J. Gill, and Q. Williams, Insights into mid-ocean ridge basalt petrogenesis; U-series disequilibria from the Siqueiros Transform, Lamont Seamounts, and East Pacific Rise, *J. Geophys. Res.*, *104*, 13,035–13,048, 1999.

Miller, R. B., The ophiolitic Ingalls Complex, north-central Cascade Mountains, Washington, *Geol. Soc. Am. Bull.*, *96*, 27–42, 1985.

Miller, R. B., and D. W. Mogk, Ultramafic rocks of a fracture-zone ophiolite, North Cascades, Washington, *Tectonophysics*, *142*, 261–289, 1987.

Nicolas, A., A melt extraction model based on structural studies in mantle peridotites, *J. Petrol.*, *27*, 999–1022, 1986.

Nicolas, A., Melt extraction from mantle peridotites: Hydrofracturing and porous flow with consequences for oceanic ridge activity, in *Magma Transport and Storage*, edited by M. P. Ryan, pp. 159–174, John Wiley, New York, 1990.

Nicolas, A., and M. Jackson, High temperature dikes in peridoties: Origin by hydraulic fracturing, *J. Petrol.*, *23*, 568–582, 1982.

Nicolas, A., and M. Rabinowicz, Mantle flow pattern at oceanic spreading centres: Relation with ophiolitic and oceanic structures, in *Ophiolites and Oceanic Lithosphere, Geol. Soc. London Spec. Publ.*, *13*, 147–151, 1984.

O'Hara, M. J., Primary magmas and the origin of basalts, *Scot. J. Geol.*, *1*, 19–40, 1965.

Ortoleva, P., J. Chadam, E. Merino, and A. Sen, Geochemical self-organization, II, The reactive-infiltration instability, *287*, 1008–1040, 1987.

Phipps Morgan, J., Melt migration beneath mid-ocean spreading centers, *Geophys. Res. Lett.*, *14*, 1238–1241, 1987.

Pollard, D. D., and P. Segall, Theoretical displacements and stresses near fractures in rock with applications to faults, joints, veins, dikes and solution surfaces, in *Fracture Mechanics of Rock*, edited by B. K. Atkinson, pp. 277–349, Academic, San Diego, Calif., 1987.

Rabinowicz, M., A. Nicholas, and J. L. Vigneresse, A rolling mill effect in asthenosphere beneath oceanic spreading centers, *Earth Planet. Sci. Lett.*, *67*, 97–108, 1984.

Renshaw, C. E., and D. D. Pollard, Numerical simulation of fracture set formation: A fracture mechanics model consistent with experimental observations, *J. Geophys. Res.*, *99*, 9359–9372, 1994.

Schreiner, W., F. Neumann, M. Neumann, R. Karch, A. End, and S. M. Roedler, Limited bifurcation assymetry in coronary arterial tree models generated by constrained constructive optimization, *J. Gen. Physiol.*, *109*, 129–140, 1997.

Segall, P., and D. D. Pollard, Joint formation in granitic

rock of the Sierra Nevada, *Geol. Soc. Am. Bull.*, *94*, 563–575, 1983.

Sims, K. W. W., D. J. DePaolo, M. T. Murrell, W. S. Baldridge, S. J. Goldstein, and D. A. Clague, Mechanisms of magma generation beneath Hawaii and mid-ocean ridges: Uranium/thorium and samarium/neodymium isotopic evidence, *Science*, *267*, 508–512, 1995.

Slater, L., M. Jull, D. McKenzie, and K. Gronvold, Deglaciation effects on mantle melting under Iceland: Results from the northern volcanic zone, *Earth Planet. Sci. Lett.*, *164*, 151–164, 1998.

Sleep, N. H. Tapping of magmas from ubiquitous mantle heterogeneities: An alternative to mantle plumes?, *J. Geophys. Res.*, *89*, 10,029–10,041, 1984.

Sparks, D. W., and E. M. Parmentier, Melt extraction from the mantle beneath spreading centers, *Earth Planet. Sci. Lett.*, *105*, 368–377, 1991.

Spiegelman, M., Physics of melt extraction: Theory, implications and applications, *Philos. Trans. R. Soc. London, Ser. A*, *342*, 23–41, 1993.

Spiegelman, M., and P. Kenyon, The requirements for chemical disequilibrium during magma migration, *Earth Planet. Sci. Lett.*, *109*, 611–620, 1992.

Spiegelman, M., and D. McKenzie, Simple 2-D models for melt extraction at mid-ocean ridges and island arcs, *Earth Planet. Sci. Lett.*, *83*, 137–152, 1987.

Spiegelman, M., P. B. Kelemen, and E. Aharonov, Causes and consequences of flow organization during melt transport: The reaction infiltration instability, *J. Geophys. Res.*, in press, 2000.

Stolper, E., A phase diagram for mid-ocean ridge basalts: Preliminary results and implications for petrogenesis, *Contrib. Mineral. Petrol.*, *74*, 13–27, 1980.

Suhr, G., Melt migration under oceanic ridges: Inferences from reactive transport modelling of upper mantle hosted dunites, *J. Petrol.*, *40*, 575–599, 1999.

Tokunaga, E., Consideration on the composition of drainage networks and their evolution, *Geograph. Rep. Tokyo Metro. Univ.*, *13*, 1–27, 1978.

Turcotte, D. L., *Fractals and Chaos in Geology and Geophysics*, 2nd ed., 398 pp., Cambridge Univ. Press, New York, 1997.

Vera, E. E., J. C. Mutter, P. Buhl, J. A. Orcutt, A. J. Harding, M. E. Kappus, R. S. Detrick, and T. M. Brocher, The structure of 0- to 0.2-m.y.-old oceanic crust at 9 degrees N on the East Pacific Rise from expanded spread profiles, *J. Geophys. Res.*, *95*, 15,529–15,556, 1990.

Volpe, A. M., and S. J. Goldstein, $^{226}Ra/^{230}Th$ disequilibrium in axial and off-axis mid-ocean ridge basalts, *Geochim. Cosmochim. Acta*, *57*, 1233–1241, 1993.

Wilson, T. A., Design of the bronchial tree, *Nature*, 668–669, 1967.

Zimmerman, M. E., D. L. Kohlstedt, and S.-I. Karato, Melt distribution in mantle rocks deformed in shear, *Geophys. Res. Lett.*, *26*, 1505–1508, 1999.